Solution of Equations Describing Fluid–Solid Reactions in Packed Columns

Neil Fernandes and George R. Gavalas
Div. of Chemistry and Chemical Engineering, California Institute of Technology, Pasadena, CA 91125

A semianalytical technique is presented for solving the equations describing an isothermal, irreversible reaction of a trace component in a packed bed of a solid reactant or adsorbent. The reaction-rate expression is assumed to have an arbitrary dependence on the solid reactant concentration, but a first-order dependence on the trace gas component. The technique relies on an integral transformation that reduces the set of partial differential equations to a set of two coupled ordinary differential equations in the spatial variables. Solving these two equations is simpler than solving the original equations by finite differences or finite elements, especially in the presence of steep concentration gradients. Two examples presented illustrate the technique: a progressive conversion model with reaction occurring at dispersed sites within the adsorbent pellet and a reaction proceeding in the shrinking core mode.

Introduction

Adsorption or reaction in packed beds of solid reactants or sorbents is widely employed for the separation or purification of gases. The modeling of adsorption in packed beds has been treated extensively, and the textbooks of Ruthven (1984) and Yang (1987) provide an excellent introduction and detailed references.

We consider here the following equations describing the isothermal adsorption or reaction of a single trace component in a packed bed:

$$D_L \frac{\partial^2 c}{\partial x^2} - u\frac{\partial c}{\partial x} - \frac{\partial c}{\partial t} = \frac{(1-\epsilon)}{\epsilon}\frac{\partial q}{\partial t}. \tag{1}$$

This equation was solved analytically by Rasmuson and Neretnieks (1980) for the case where the sink term, $(\partial q/\partial t)$, was controlled by the external film resistance and intraparticle diffusion, with adsorption–desorption at equilibrium and a linear adsorption isotherm. The case of a nonlinear isotherm has been treated numerically by Liapis and Rippin (1978), among others. To our knowledge no analytical solution is available for irreversible adsorption or reaction, with dispersed flow models.

In this article we extend a semianalytical technique of Del Borghi et al. (1976) and Dudukovic and Lamba (1978) for fluid–solid reactions in single pellets to reactions in packed beds. This technique involves the transformation of the governing partial differential equations (PDEs) into two coupled ordinary differential equations (ODEs). The technique is restricted to isothermal, irreversible reactions, first order with respect to the gaseous reactant. These conditions often apply when trace quantities of gaseous contaminants are removed by irreversible reactions or chemisorption. An example is the removal of hydrogen sulfide by reaction in a bed of iron or zinc oxide. The governing equations are similar to those of reversible adsorption and are amenable to numerical solution by collocation methods such as those used by Liapis and Rippin. The technique proposed here is simpler and numerically more efficient, especially when steep concentration gradients are encountered inside the pellets or along the bed.

Analytical Development

We consider a fluid–solid reaction

$$\nu_A A(f) + \nu_B B(s) \rightarrow \nu_P P(f) + \nu_Q Q(s) \tag{2}$$

with rate per unit solid volume given by

$$R = kf(X)c', \tag{3}$$

where c' is the concentration of the fluid component A per unit fluid volume in the pellet and X is the local conversion

of the solid B. The form of the function f can be derived from various reaction models or it can be empirically determined.

The conservation equations for A and B for a bed of spherical pellets can be written as

$$D_L\frac{\partial^2 c}{\partial x^2}-u\frac{\partial c}{\partial x}=\frac{(1-\epsilon)}{\epsilon}\frac{3k_m}{R_p}(c-c'|_{R_p}) \tag{4}$$

$$x=0:\quad uc_0G(t)=uc-D_L\frac{\partial c}{\partial x} \tag{5}$$

$$x=L:\quad \frac{\partial c}{\partial x}=0 \tag{6}$$

$$D_e\frac{\partial}{\partial r}\left(r^2\frac{\partial c'}{\partial r}\right)=\nu_A k f(X)c' \tag{7}$$

$$r=0:\quad \frac{\partial c'}{\partial r}=0 \tag{8}$$

$$r=R_p:\quad D_e\frac{\partial c'}{\partial r}=k_m(c-c') \tag{9}$$

$$\frac{\partial X}{\partial t}=\nu_B k f(X)c' \tag{10}$$

$$t=0:\quad X=0. \tag{11}$$

These equations incorporate the following simplifications and assumptions:

1. The gas-phase accumulation terms in the bed and pellet equations, Eqs. 4 and 7, have been neglected since in the adsorption/reaction of trace gases, the ratio of bulk gas concentration to solid reactant concentration (c_0/σ_0) is very small, in many cases below 10^{-3}. For example, a copper-exchanged zeolite, 13-X containing 3 wt. % Cu, that is, σ_0 about 0.7×10^{-3} mol/cm^{-3}, can be used to desulfurize a flue gas with 0.5% SO_2. At 300°C the SO_2 concentration is $c_0=1.06\times10^{-3}$ mol/cm^{-7} so that $c_0/\sigma_0\simeq1.5\times10^{-4}$.

2. The size and porous structure of the pellets do not change with reaction, excluding from consideration reactions such as lime sulfation that significantly decrease the pore volume.

3. Through the function $G(t)$ in Eq. 5, time varying inlet concentrations have been included in the formulation of this problem. However, $G(t)$ must change relatively slowly for consistency with the approximation 1 above.

Defining the dimensionless variables

$$\xi=\frac{x}{R_p},\quad \rho=\frac{r}{R_p},\quad \zeta=\frac{c'}{c_0},\quad y=\frac{c}{c_0},\quad \tau=\nu_B\frac{kc_0t}{\sigma_0}$$

and the dimensionless parameters

$$Pe=\frac{uR_p}{D_L},\quad \beta=\frac{(1-\epsilon)}{\epsilon}\frac{3k_mR_p}{D_L},$$

$$\Phi^2=\frac{\nu_A kR_p^2}{D_e},\quad Bi_m=\frac{k_mR_p}{D_e}$$

the equations take the dimensionless form

$$\frac{\partial^2 y}{\partial\xi^2}-Pe\frac{\partial y}{\partial\xi}=\beta(y-\zeta|_{\rho=1}) \tag{12}$$

$$\xi=0:\quad g(\tau)=y-\frac{1}{Pe}\frac{\partial y}{\partial\xi} \tag{13}$$

$$\xi=\Lambda:\quad \frac{\partial y}{\partial\xi}=0 \tag{14}$$

$$\frac{1}{\rho^2}\frac{\partial}{\partial\rho}\left(\rho^2\frac{\partial\zeta}{\partial\rho}\right)=\Phi^2f(X)\zeta \tag{15}$$

$$\rho=0:\quad \frac{\partial\zeta}{\partial\rho}=0 \tag{16}$$

$$\rho=1:\quad \frac{\partial\zeta}{\partial\rho}=Bi_m(y-\zeta) \tag{17}$$

$$\frac{\partial X}{\partial\tau}=f(X)\zeta \tag{18}$$

$$\tau=0:\quad X=0. \tag{19}$$

The basic transformation consists of replacing the dependent concentration variable ζ by the cumulative pellet concentration

$$z=\int_0^\tau\zeta\,d\tau'. \tag{20}$$

Dividing Eq. 18 by $f(X)$ and integrating yields the following relation between z and X:

$$z=\int_0^X\frac{dx}{f(x)}. \tag{21}$$

Equation 21 defines X implicitly as a function of z

$$X=w(z). \tag{22}$$

Integrating Eqs. 15–17 with respect to time, we obtain the corresponding equations in the cumulative concentration z:

$$\frac{1}{\rho^2}\frac{\partial}{\partial\rho}\left(\rho^2\frac{\partial z}{\partial\rho}\right)=\Phi^2w(z) \tag{23}$$

$$\rho=0:\quad \frac{\partial z}{\partial\rho}=0 \tag{24}$$

$$\rho=1:\quad \frac{\partial z}{\partial\rho}=Bi_m(Y-z), \tag{25}$$

where Y is the cumulative column concentration

$$Y=\int_0^\tau y(\xi,\tau')\,d\tau'. \tag{26}$$

In deriving Eq. 23 we made use of the relation

$$w(z) = X = \int_0^\tau f(X)\zeta(\rho, \tau')\, d\tau',$$

obtained by direct integration of Eq. 18. It is noted that the elimination of the dependent variable X from Eq. 23 is possible only when the chemical reaction is first order in the gas concentration.

The solution to the two-point boundary problem 23–25 can be obtained numerically by integrating Eq. 23 from the center of the pellet to the surface using the initial conditions

$$\rho = 0: \quad \frac{\partial z}{\partial \rho} = 0; \quad z = \kappa \tag{27}$$

for different values of κ and then using boundary condition 25 to establish a one-to-one correspondence between Y and z at $\rho = 1$:

$$z(1, Y) = h(Y). \tag{28}$$

It is often useful to know the fraction of the sorbent that remains unreacted at breakthrough. In order to extract this information from the transformed equations, it is necessary to know the extent of conversion of the pellets as a function of Y. This can be found by integrating Eq. 22 throughout the pellet

$$\sigma_{av}(Y) = 3\int_0^1 \rho^2(1 - w(z))\, d\rho, \tag{29}$$

where it is recalled that $z = z(\rho, Y)$. The functions $h(Y)$ and $\sigma_{av}(Y)$ summarize all the information contained in the pellet equations. The numerical solution provides $h(Y)$ and $\sigma_{av}(Y)$ at a discrete set of points, which can be interpolated using cubic splines to provide smooth functions.

Proceeding to the column problem, Eqs. 12–14 are integrated with respect to τ, yielding

$$\frac{\partial^2 Y}{\partial \xi^2} - Pe\frac{\partial Y}{\partial \xi} = \beta(Y - h(Y)) \tag{30}$$

$$\xi = 0: \quad \int_0^\tau g(t)\, dt = Y - \frac{1}{Pe}\frac{\partial Y}{\partial \xi} \tag{31}$$

$$\xi = \Lambda: \quad \frac{\partial Y}{\partial \xi} = 0. \tag{32}$$

Using the initial conditions

$$\xi = \Lambda: \quad \frac{\partial Y}{\partial \xi} = 0; \quad Y = \lambda, \tag{33}$$

Equation 30 is integrated from $\xi = \Lambda$ to $\xi = 0$ for different values of λ. Each value of λ yields $Y(0, \tau)$ and $(\partial Y/\partial \xi)(0, \tau)$ as well as the cumulative concentration profile $Y(\xi, \tau)$. The boundary quantities are substituted into Eq. 31 to obtain the time τ for this particular profile. From the profile $Y(\xi, \tau)$ and the function $\sigma_{av}(Y)$, the concentration of solid reactant is immediately known everywhere in the column. To find the gas concentration profiles $y(\xi, \tau)$, the cumulative profiles $Y(\xi, \tau)$ could be numerically differentiated. However, the numerical integration of Eqs. 30–32 would yield Y at a nonequidistant set of values of τ, so that in practice it would be necessary to calculate the cumulative concentration profiles for a very dense set of values of τ to allow accurate numerical differentiation. A more efficient procedure becomes apparent by differentiating Eq. 30 with respect to τ to obtain the linear equation

$$\frac{\partial^2 y}{\partial \xi^2} - Pe\frac{\partial y}{\partial \xi} = \beta[1 - h'(Y)]y, \tag{34}$$

subject to the boundary conditions 13 and 14. Equation 34 is linear because $h'(Y)$ is a known function of ξ through the cumulative concentration profile $Y(\xi, \tau)$. The function $h'(Y)$ can be obtained from the spline formulas used to generate $h(Y)$, but a more accurate method is given in the Appendix. By integrating Eq. 34 from $\xi = \Lambda$ to $\xi = 0$ with the initial conditions

$$\xi = \Lambda: \quad \frac{\partial y}{\partial \xi} = 0; \quad y = \alpha, \tag{35}$$

a profile is obtained that differs from the true concentration profile only by a scaling factor. This profile can be scaled by a suitable constant so that the result $y(\xi, \tau)$ satisfies boundary condition 13.

It is useful at this point to summarize the computational procedure required to solve the original problem. First, the functions $h(Y)$ and $\sigma_{av}(Y)$ are calculated from the single-pellet equations. In general, this involves solving the differential Eq. 23 for several different values of $z(0, Y) = \kappa$. For certain fluid–solid reaction models the calculation of these functions may require solution of an algebraic equation rather than the differential Eq. 23 (Example 2). Proceeding to the column equations, Eqs. 30 and 34 need to be solved once for every concentration profile required. There is no requirement for a time mesh as with finite difference methods. One can solve for as few profiles as are needed to accurately portray the breakthrough behavior of the column.

Example 1

The technique will now be illustrated for an irreversible reaction that is first order in both the gaseous reactant and the reacting sites in the solid. In this case the function f takes the simple form

$$f(X) = 1 - X,$$

where the initial density of reacting sites is absorbed into the rate constant k. Equations 21 and 22 now appear as

$$X = w(z) = 1 - e^{-z}.$$

The relevant forms of Eqs. 23–25 were integrated by a Runge–Kutta method with adaptive step-size control (RKAS)

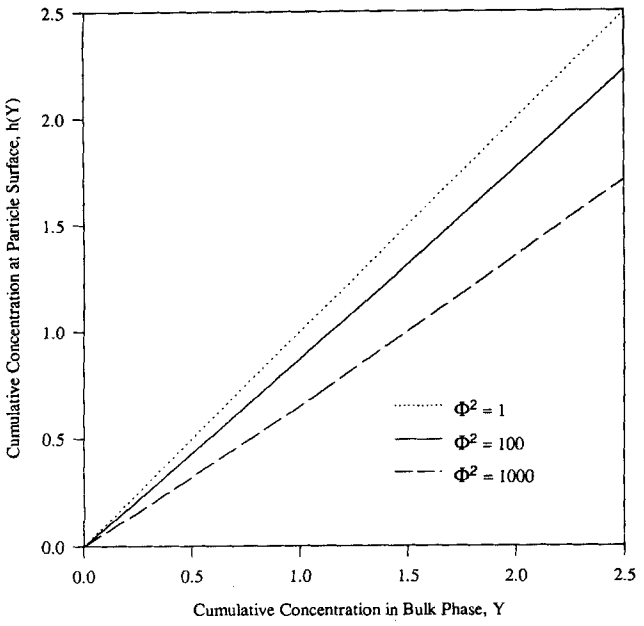

Figure 1. Function $h(Y)$ in example 1 for $Bi_m = 50$ for various values of Φ^2.

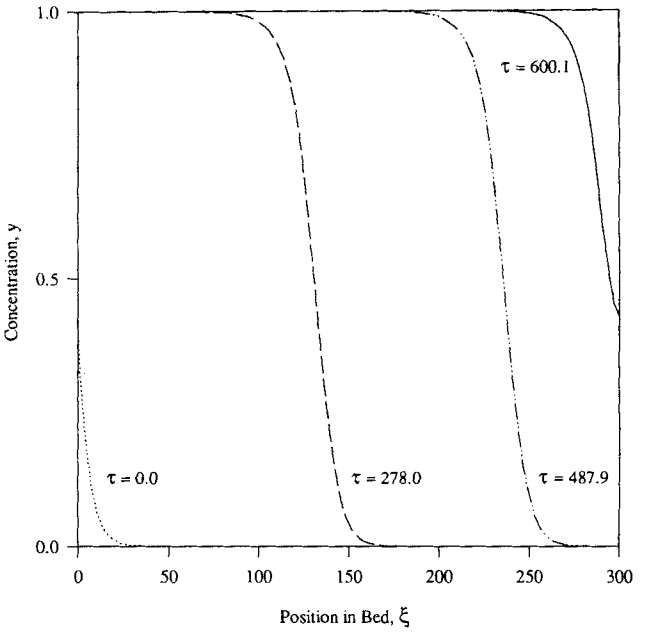

Figure 3. Development of the concentration profiles $y(\xi, \tau)$ in example 1 for $\Phi^2 = 100$, $Bi_m = 50$, $Pe = 1.1$, $\beta = 3.3$.

to calculate the function $h(Y)$. Figure 1 shows the calculated $h(Y)$ for various values of Φ. In practical applications, the mass-transfer Biot number is sufficiently high and most resistance is due to intraparticle processes. For small values of Φ, intraparticle gradients are small and thus the cumulative concentrations in the bulk, Y, and at the particle surface, $h(Y)$, are similar. For large values of Φ, Y is significantly larger than $h(Y)$, as shown in Figure 1. Figures 2 through 6 survey the results easily extracted through this method of solution. Figures 2, 3 and 4 illustrate the development of the gas and solid concentration profiles in the bed. Note how the gas and solid concentration profiles at $\tau = 0.0$ in Figures 3 and 4 are consistent with the pseudo-steady-state assumption. Figure 3 reveals the wavelike character of the solution reflecting the relatively small effect of dispersive processes. Finally, Figures 5 and 6 show breakthrough curves for different values of various parameters. For the range of parame-

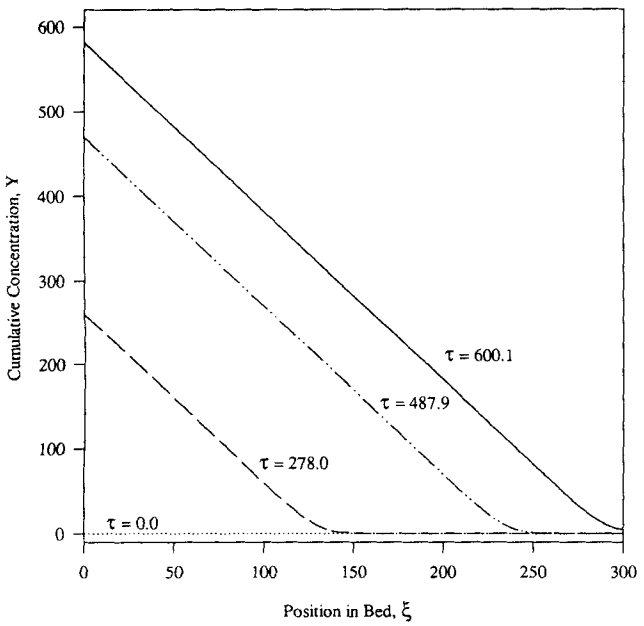

Figure 2. Development of the cumulative concentration profiles $Y(\xi, \tau)$ in example 1 for $\Phi^2 = 100$, $Bi_m = 50$, $Pe = 1.1$, $\beta = 3.3$.

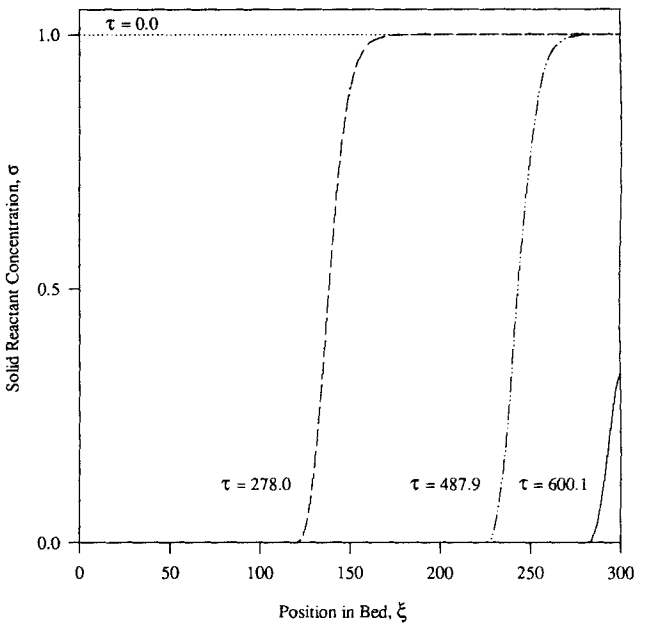

Figure 4. Concentration profiles of the solid reactant in example 1 for $\Phi^2 = 100$, $Bi_m = 50$, $Pe = 1.1$, $\beta = 3.3$.

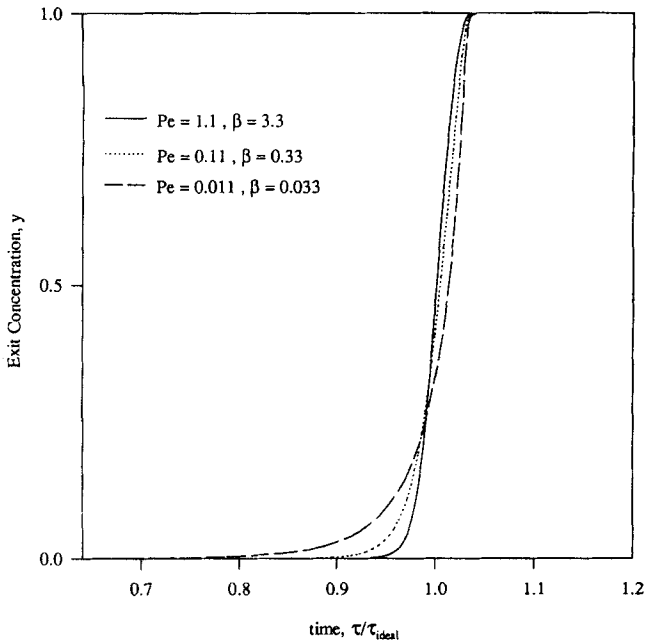

Figure 5. Effect of axial dispersion on the breakthrough curve in example 1 for $\Phi^2 = 100$, $Bi_m = 50$, $L = 300$.

ters explored, broadening effects caused by kinetic resistances in the pellet are seen to be much more important than those due to axial dispersion.

In this example the feed concentration to the column was taken as constant. However, the technique can be applied to unsteady inputs, subject to the restrictions of the pseudo-steady-state approximation. In particular, the characteristic time for changes in the feed concentration must be much larger than the characteristic time for concentration changes in the column and the pellet. Our experience with Example 1 indicates that the solution of Eq. 34 is very sensitive to the function $h'(Y)$. Differentiation of the spline-interpolated function Y introduces sizable error, especially for Thiele moduli below 1 or above 20. However, this difficulty was largely eliminated by using the direct calculation of $h'(Y)$ outlined in the Appendix. To test the numerical accuracy of the technique, the numerical solution for short times was compared with the corresponding analytical solution obtained from the asymptotic form of Eq. 34,

$$\frac{\partial^2 y}{\partial \xi^2} - Pe\frac{\partial y}{\partial \xi} = \beta A(Bi_m, \Phi),$$

where $A(Bi_m, \Phi)$ is a constant calculated from the short-time limiting form of the pellet equations. The two solutions differed by less than 1%. Overall mass balances based on the outlet tracer concentration-time curve also gave consistent results.

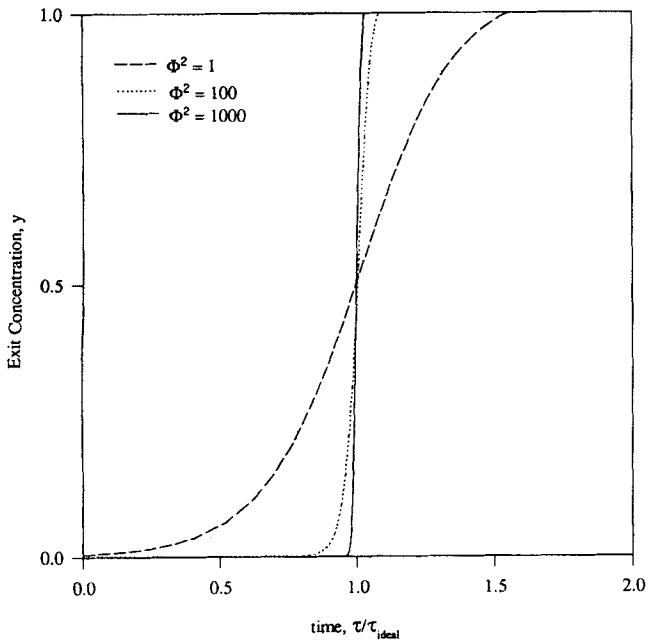

Figure 6. Effect of reaction rate constant on the shape of the breakthrough curve in example 1 for $Bi_m = 50$, $Pe = 1.1$, $\beta = 3.3$, $L = 300$.

Example 2

As pointed out earlier, functions $h(Y)$ and $\sigma_{av}(Y)$ can be calculated for a variety of reaction models. To further illustrate this calculation, we consider a pellet undergoing shrinking core reaction. Mass transfer through the gas film, diffusion through the product layer, and reaction at the interface are described by the standard pseudo-steady-state equations

$$r_c < r < R_p: \quad \frac{D_e}{r^2}\frac{\partial}{\partial r}\left(r^2\frac{\partial c'}{\partial r}\right) = 0 \tag{36}$$

$$r = r_c: \quad D_e\frac{\partial c'}{\partial r} = \nu_A k c' \tag{37}$$

$$r = R_p: \quad k_m(c - c') = D_e\frac{\partial c'}{\partial r} \tag{38}$$

$$\frac{d}{dt}\left(\sigma_0\frac{4}{3}\pi r_c^3\right) = -\nu_B k c' 4\pi r_c^2 \tag{39}$$

$$t = 0: \quad r_c = R_p, \tag{40}$$

where c' is the concentration of the gaseous reactant, σ_0 is the concentration of the solid reactant in the core, and r_c, R_p are the radii of the core and the pellet. With the new definition of dimensionless time

$$\tau = \frac{\nu_B k c_0}{\sigma_0 R_p} t$$

and Thiele modulus

$$\Phi^2 = \frac{\nu_A k R_p}{D_e},$$

Equations 36–38 yield the following expressions for the dimensionless gradients at the core surface and pellet surface

$$\rho = \rho_c: \quad \frac{\partial \zeta}{\partial \rho} = \frac{\zeta(1,\tau) - \zeta(\rho_c,\tau)}{\rho_c(1-\rho_c)} \tag{41}$$

$$\rho = 1: \quad \frac{\partial \zeta}{\partial \rho} = \frac{\rho_c[\zeta(1,\tau) - \zeta(\rho_c,\tau)]}{(1-\rho_c).} \tag{42}$$

Equation 41 is now introduced into the dimensionless form of Eq. 39 to obtain

$$\frac{\partial \rho_c}{\partial \tau} = \frac{-\zeta(1,\tau)}{\Phi^2(1-\rho_c)\rho_c + 1} = -\zeta(\rho_c,\tau). \tag{43}$$

After integration with respect to time, Eq. 43 appears in the familiar form

$$\Phi^2\left(\frac{\rho_c^2}{2} - \frac{\rho_c^3}{3} - \frac{1}{6}\right) + \rho_c - 1 = -z(1,Y). \tag{44}$$

Matching the fluxes at the solid-fluid boundary gives

$$\rho = 1: \quad (Y - z) = \frac{1}{Bi_m}\int_0^\tau \frac{\rho_c}{1-\rho_c}[\zeta(1,\tau') - \zeta(\rho_c,\tau')]\,d\tau', \tag{45}$$

which after substitution with Eq. 43 and integration, provides the simple equation

$$Bi_m[Y - z(1,Y)] = \frac{\Phi^2}{3}(1-\rho_c^3). \tag{46}$$

Equations 44 and 46 can be easily solved for ρ_c and $z(1, Y)$. For example, a value for z is selected and Eq. 44 is solved for ρ_c, where only the root between 0 and 1 is physically relevant. The values of z and ρ_c are then substituted into Eq. 46 to give the corresponding Y. With Y, $z(1, Y)$, and ρ_c all known, one immediately has

$$h(Y) = z(1,Y) \tag{47}$$

$$\sigma_{av}(Y) = \rho_c^3. \tag{48}$$

As before cubic splines can be used to generate continuous functions. Figure 7 shows breakthrough curves calculated for the progressive conversion model and the shrinking core models for high values of the Thiele modulus. In this case, both models describe the same physical situation, namely reactions with steep intraparticle concentration gradients, and as expected the two breakthrough curves are in close agreement.

A further special case of some interest is one in which the reactive solid consists of small crystallites supported on an inert porous matrix. The mathematical structure of this problem is similar to that of the grain model. If reaction in the crystallites takes place in the shrinking core fashion, then the analysis of Example 2 can be combined with that of Example 1 to provide the function $h(Y)$ for the pellet. The function $h(Y)$ of the pellet is then used in the column equations. This procedure represents a compounding from one level to the next one: from the crystallite to the pellet and from the pellet to the column. Each such transition, from one level to the next, eliminates one spatial coordinate. For background material on shrinking-core and grain models, see Levenspiel (1972) and Szekely and Evans (1971).

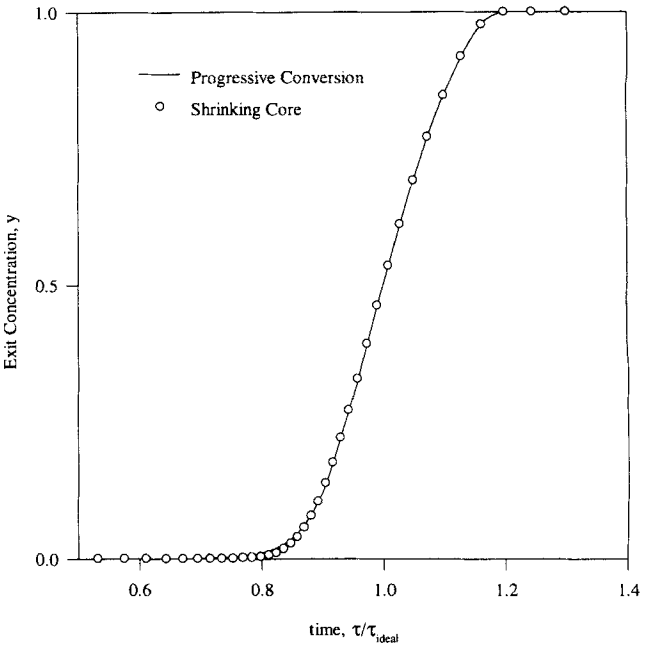

Figure 7. Breakthrough curves for the progressive conversion model, and the shrinking core model of example 2 for $\Phi^2 = 1{,}000$, $Bi_m = 50$, $Pe = 0.11$, $\beta = 0.33$, $L = 300$.

Discussion and Conclusions

A previous technique of Del Borghi et al. (1976) and Dudukovic and Lamba (1978) dealing with a single spatial variable (single pellet) has been extended to the case of two spatial variables (packed bed). This technique allows successive elimination of spatial variables from the smaller scale to the larger scale until only the spatial variable at the highest level remains. Time is eliminated as an independent variable and becomes a parameter so that there is no need for a mesh in this variable. Once the function $h(Y)$ has been computed for the pellet, only two one-dimensional spatial integrations are required for each time at which the solution is desired.

Transformation of the original partial differential equations to ordinary differential equations is advantageous because of the availability of very efficient numerical algorithms for the latter, especially when the solutions have steep gradients. For example, the fourth-order RKAS algorithm automatically reduces the integration step to handle steep gradients in the dependent variable. In typical finite-element and finite-difference techniques very dense meshes in time and space must be used in the vicinity of steep concentration fronts. Although moving finite-element techniques have been developed to handle such problems, their implementation is considerably more tedious. The technique presented here is applicable only to a limited class of problems involving irreversible reactions, first order in the gaseous reactant, and ex-

cludes reactions that significantly change the porous structure of the reacting solid.

Acknowledgment

Funding for this project was provided by the Advanced Development Activity for Microgravity Containerless Technology of the Jet Propulsion Laboratory.

Notation

Bi_m = pellet mass-transfer Biot number
c = gas concentration in the bulk phase
c^1 = gas concentration in the pellet
D_e = effective diffusivity within the pellet
D_L = axial dispersion coefficient within the column
h' = derivative of h with respect to Y
k_m = mass-transfer coefficient
L = total length of packed bed
Pe = pellet Peclet number
q = concentration of solid product in the pellet
r = radial distance in pellet
u = interstitial velocity
x = axial distance from front of bed
y = dimensionless bulk concentration
z = cumulative concentration in the pellet

Greek letters

ϵ = bed void fraction
ξ = dimensionless distance from front of bed
ζ = dimensionless gas concentration within the pellet
Λ = dimensionless total bed length, L/R_p
ρ = dimensionless radial distance within pellet
ρ_c = dimensionless unreacted core radius
σ_{av} = pellet average of the solid reactant concentration
τ = dimensionless time
τ_{ideal} = dimensionless ideal breakthrough time

Literature Cited

Del Borghi, M., J. C. Dunn, and K. B. Bischoff, "A Technique for Solution of the Equations for Fluid Solid Reactions with Diffusion," *Chem. Eng. Sci.*, **31**, 1065 (1976).

Dudukovic, M. P., and H. S. Lamba, "Solution of Moving Boundary Problems for Gas-Solid Noncatalytic Reactions by Orthogonal Collocation," *Chem. Eng. Sci.*, **33**, 303 (1978).

Levenspiel, O., *Chemical Reaction Engineering*, Wiley, New York (1972).

Liapis, A. I., and D. W. T. Rippin, "The Simulation of Binary Adsorption in Activated Carbon Columns using Estimates of Diffusional Resistance within the Carbon Particles Derived from Batch Experiments," *Chem. Eng. Sci.*, **33**, 593 (1978).

Rasmuson, A., and I. Neretnieks, "Exact Solution for Diffusion in Particles and Longitudinal Dispersion in Packed Beds," *AIChE J.*, **26**, 686 (1980).

Ruthven, D. M., *Principles of Adsorption and Adsorption Processes*, Wiley, New York (1984).

Szekely, J., and J. W. Evans, "The Effect of Grain Size, Porosity and Temperature on the Reaction of Porous Pellets," *Chem. Eng. Sci.*, **26**, 1901 (1971).

Yang, R. T., *Gas Separation by Adsorption Processes*, Butterworths, Boston (1987).

Appendix

A more accurate method for calculating $h'(Y)$ for the progressive conversion problem is as follows. The pellet equations for the cumulative concentration are

$$\frac{1}{\rho^2}\frac{\partial}{\rho}\left(\rho^2\frac{\partial z}{\partial \rho}\right) = \Phi^2 w(z) \tag{A1}$$

$$\rho = 0: \quad \frac{\partial z}{\partial \rho} = 0 \tag{A2}$$

$$\rho = 1: \quad \frac{\partial z}{\partial \rho} = Bi_m(Y - z). \tag{A3}$$

These equations can be differentiated with respect to Y to obtain an equation in the derivative $v = \partial z/\partial Y$:

$$\frac{1}{\rho^2}\frac{\partial}{\rho}\left(\rho^2\frac{\partial v}{\partial \rho}\right) = \Phi^2 w'(z)v \tag{A4}$$

$$\rho = 0: \quad \frac{\partial v}{\partial \rho} = 0 \tag{A5}$$

$$\rho = 1: \quad Bi_m(1 - v) = \frac{\partial v}{\partial \rho}. \tag{A6}$$

With z known from the solution of A1–A3, Eqs. A4–A6 constitute a linear boundary value problem in v and can be readily integrated. We have found that calculating v from Eqs. A4–A6 gives much more accurate results than those obtained by numerically differentiating $h(Y)$, especially for early times.

For the shrinking-core model, significantly less work is involved. The pertinent equations from the main text are

$$\Phi^2\left(\frac{\rho_c^2}{2} - \frac{\rho_c^3}{3} - \frac{1}{6}\right) + \rho_c - 1 = -z(1, Y) \tag{A7}$$

$$Bi_m[Y - z(1, Y)] = \frac{\Phi^2}{3}(1 - \rho_c^3), \tag{A8}$$

which result, respectively, from solving for the reaction front in the pellet and continuity of reactant flux at the pellet surface. By differentiating Eqs. A7 and A8 with respect to Y and solving for $(\partial z/\partial Y)|_{\rho=1}$, the result is

$$\frac{\partial z}{\partial Y}\Big|_{\rho=1} = \frac{1}{\left[1 + \dfrac{\Phi^2\rho_c^2}{Bi_m\Phi^2\rho_c(1 - \rho_c) + 1}\right]}$$

Manuscript received Aug. 22, 1994, and revision received Dec. 22, 1994.